Lattice Boltzmann modeling of thermal conduction in composites with thermal contact resistance

Chiyu Xie[1], Jinku Wang[2], Dong Wang[3], Ning Pan[4], Moran Wang[1,3†]

[1]*Department of Engineering Mechanics and CNMM, Tsinghua University, Beijing 100084, China;*

[2]*National Institute of Metrology, Beijing 100084, China*

[3] *School of Materials Science, Wuhan Textile University, Wuhan ,Hubei 430200, China*

[4]*Nanomaterials in Environment, Agriculture & Technology (NEAT), University of California, Davis, CA 95616, USA*

Abstract: The effective thermal conductivity of composite materials with thermal contact resistance at interfaces is studied by lattice Boltzmann modeling in this work. We modified the non-dimensional partial bounce-back scheme, proposed by Han et al. [*Int. J. Thermal Sci., 2008. **47**: 1276-1283*], to introduce a real thermal contact resistance at interfaces into the thermal lattice Boltzmann framework by re-deriving the redistribution function of heat at the phase interfaces for a corrected dimensional formulation. The modified scheme was validated in several cases with good agreement between the simulation results and the corresponding theoretical solutions. Furthermore, we predicted the effective thermal conductivities of composite materials using this method where the contact thermal resistance was not negligible, and revealed the effects of particle volume fraction, thermal contact resistance and particle size. The results in this study may provide a useful support for materials design and structure optimization.

***Keywords*:** lattice Boltzmann method; partial bounce-back scheme; thermal contact resistance; effective thermal conductivity

How to cite this article:

Chiyu Xie, Jinku Wang, Dong Wang, Ning Pan and Moran Wang (2015). Lattice Boltzmann Modeling of Thermal Conduction in Composites with Thermal Contact Resistance. Communications in Computational Physics, 17, pp 1037-1055 doi:10.4208/cicp.2014.m360

† Corresponding author; Email: mrwang@tsinghua.edu.cn

1. Introduction

It is well known that the thermal contact resistance (TCR) is caused by the low-conductivity interfacial gap between two contact surfaces, which has significant impact in many engineering applications, such as electronic packaging [1, 2] and composite materials manufacture and design [3, 4]. Because of the often tiny scale and complex shape involved, experimental investigation is often cumbersome and even impossible, many efforts have been made in developing theoretical model to investigate the TCR, based on two basic surface contact modes: the conforming rough surfaces mode [5] and the nonconforming rough surfaces mode [6, 7]. However, in practical issues there are always a lot surfaces with irregular shapes in contact, such as the particle-particle contact in particle-reinforced composites. Thus comes many difficulties in predicting the thermal properties of these composites when the inner TCR is concerned. To the best of our knowledge, few remedies are available to deal with this thorny problem, and numerical methods have therefore become the alternative.

In recent years, the lattice Boltzmann method (LBM) has been developed into a successful numerical scheme for fluid flow simulation [8, 9]. Compared with the traditional CFD methods, LBM has advantages especially for applications involving large number of interfaces or/and complex geometries. Besides for hydrodynamics, efforts have also been made to apply LBM to solving various fluid transport problems coupled with electrokinetics, magnetic, thermodynamics or even chemical reactions [10-17]. Attempts have been made in using LBM to study the interfacial heat transfer process, and a few models have been developed in the lattice Boltzmann method for simulation of the thermo-hydrodynamics since 1993 [18-25]. More specifically, a single distribution function model was introduced into the lattice Boltzmann method to simulate the Rayleigh-Bénard convection. It was however admitted that with severe numerical instability, the applicable temperature range is limited to a narrow scope [18-20]. To overcome the drawback, a double distribution function model was developed [21-23], in which a density distribution function is introduced to simulate the hydrodynamics (fluid flow), while an internal energy distribution function to tackle the thermodynamics (heat transfer). He et al. [23] proved that such double distribution model can appropriately treat the viscous heat dissipation and compression work done by the pressure. However, He's method is too complicated to use so that several simplified versions have been subsequently developed. For instance, Peng et al. [24] proposed a simple internal energy function evolution method for cases with negligible heat dissipation and compression work. Wang et al. [25] developed a general scheme for fluid-solid interfacial conjugate heat transfer process. Consequently, this type of method has gained wide application in predictions of effective thermal properties of engineering multiphase materials, with results validated by experimental data [26-30].

Furthermore, in analyzing macroscopic engineering materials, an important assumption is the continuity held at interfaces, i.e., thermal contact resistance is negligible. One result this assumption led to is that the effective thermal conductivity of granular porous materials increases with the decreased pore size for a given porosity [31], which agreed well with experimental data from both natural and engineering materials [32, 33]. However, some recent measurements for nanoporous materials have shown some contradictory results that the

effective thermal conductivity actually decreases with the reduced pore size [34] or particle size as in silica aerogels [35]. It is now known that the impact of all interfacial mechanisms become more significant at smaller, especially nanoscale [36, 37]. Growing importance of the thermal contact resistance and the increased number of interfaces in finer particles were ascribed to cause the conflicting predictions. Again for more accurate prediction, the thermal contact resistance has to be considered, however tough and challenging. Wang et al. [38] tackled the problem by assuming that the thermal contact resistance layers between the particles forming a network frame in a composite system so as to take the thermal contact resistance into account. However this method is limited by this assumed uniform contact resistance. Very recently, Yoshida et al. [39] proposed a prospective boundary scheme for two-phase interface: using two simple modifications of the collision and streaming process, the continuities of the physical variable and its flux are simultaneously satisfied in a transient analysis. However, the actual interfacial thermal contact resistance between two phases is still ignored. To take the thermal contact resistance into consideration more explicitly, Han et al. [40] proposed a partial bounce back (PBB) scheme for the LBM framework. Han's strategy seems promising; however, their derivation of TCR expression is dimensionally inhomogeneous and hence wrong, as discussed in detail later.

Therefore in this work, the PBB scheme will be revisited and re-derived to obtain its correct dimensional formula for TCR. After discussing its applicability, we validate the new scheme for some simple cases by comparisons with the corresponding theoretical resolutions. Furthermore, we will apply this modified scheme to predict the effective thermal conductivity of particle-reinforced composites where the TCR is non-negligible, so as to explore the major factors that influence the effective thermal properties of the materials.

2. Numerical methods

2.1 LBM scheme for thermal conduction

Consider a pure thermal conduction in a composite material without any heat source. The general governing equation (Poisson equation) for heat transfer is

$$\rho c_p \frac{\partial T}{\partial t} = \nabla \cdot (\lambda \nabla T), \tag{1}$$

where T is the temperature, ρ the density, λ the thermal conductivity which may depend on position, and c_p the specific heat capacity. To solve Eq. (1) in such multiphase system with high computational efficiency, a simplified thermal lattice Boltzmann method has been proposed [24, 25]. Accordingly the energy evolution equation can be generally given as

$$\mathrm{g}_i(\boldsymbol{x} + \boldsymbol{e}_i \delta t, t + \delta t) - \mathrm{g}_i(\boldsymbol{x}, t) = -\frac{1}{\tau_\mathrm{g}}\left[\mathrm{g}_i(\boldsymbol{x}, t) - \mathrm{g}_i^{eq}(\boldsymbol{x}, t)\right], \tag{2}$$

where g_i and g_i^{eq} are respectively the internal energy distribution function and corresponding equilibrium distribution function with discrete lattice velocity $\boldsymbol{e}_i$ along the i-th direction; δt is the time step and τ_g is the relaxation time for g_i. For a two-dimensional nine-speed (D2Q9) model, there are

$$\boldsymbol{e}_i = \begin{cases} (0,0) & i = 0 \\ (\pm 1,0)c, (0,\pm 1)c & i = 1 \; to \; 4 \\ (\pm 1,\pm 1)c & i = 5 \; to \; 8 \end{cases}, \tag{3}$$

$$g_i^{eq} = \begin{cases} 0 & i = 0 \\ \frac{1}{6}\rho c_p T & i = 1\ to\ 4 \\ \frac{1}{12}\rho c_p T & i = 5\ to\ 8\ , \end{cases} \tag{4}$$

and

$$\tau_g = \frac{3}{2}\frac{\lambda}{\rho c_p c^2 \delta t} + 0.5\ ; \tag{5}$$

while for a three-dimensional fifteen-speed (D3Q15) model, there are instead

$$\boldsymbol{e}_i = \begin{cases} (0,0,0) & i = 0 \\ (\pm 1,0,0)c, (0,\pm 1,0)c, (0,0,\pm 1)c & i = 1\ to\ 6\ , \\ (\pm 1,\pm 1,\pm 1)c & i = 7\ to\ 14 \end{cases} \tag{6}$$

$$g_i^{eq} = \begin{cases} 0 & i = 0 \\ \frac{1}{9}\rho c_p T & i = 1\ to\ 6 \\ \frac{1}{24}\rho c_p T & i = 7\ to\ 14 \end{cases}, \tag{7}$$

and

$$\tau_g = \frac{9}{5}\frac{\lambda}{\rho c_p c^2 \delta t} + 0.5\ , \tag{8}$$

where c is the lattice speed that theoretically can take any positive value only to insure the τ_g value within (0.5, 2) [25, 41]. According to Ref. [42], the temperature and the heat flux can be calculated as

$$T = \frac{1}{\rho c_p}\sum_i g_i\ , \tag{9}$$

$$\boldsymbol{q} = \left(\sum_i \boldsymbol{e}_i g_i\right)\frac{\tau_g - 0.5}{\tau_g}\ . \tag{10}$$

Finally, the effective thermal conductivity λ_{eff} can be determined by the solved temperature field:

$$\lambda_{eff} = \frac{L\int \boldsymbol{q}\cdot dA}{\Delta T\int dA}\ , \tag{11}$$

where $\boldsymbol{q}$ is the steady heat flux through the cross section area dA between the temperature difference ΔT with a distance L.

Thus the unsteady heat conduction described by Eq. (1) can be described and solved through such a form of energy evolution in the framework of Eqs. (2-10), termed as thermal lattice Boltzmann method (TLBM). Then, steady-state heat conduction can be simply treated as a special case when the time-dependent term vanishes.

The critical issue here however is the ambiguity which one is the solved property, thermal conductivity (λ) or thermal diffusivity (a =$\lambda/\rho c_p$). An expedient solution for this problem was to assume ρc_p = 1 [26, 43], so that λ is numerically equal to a. This assumption ρc_p = 1 has been adopted widely and works well for cases with negligible thermal contact resistance [26-30, 44]. However when the temperature and heat flux at

interfaces have to be considered, the assumption ($\rho c_p = 1$) may lead to conflict so that the entire framework needs to be reformulated.

Therefore, for steady-state heat conduction in a multi-component system, the time-dependent term vanished and Eq. (1) reduces into the simple Laplace-like equation,

$$\nabla \cdot \left(\tilde{\lambda} \nabla T\right) = 0. \tag{12}$$

To proceed within the thermal lattice Boltzmann framework, it can be treated as the *temperature* "diffusing" through the multiphase lattice system. The position-dependent temperature diffusivity, $\tilde{\lambda}$, has the same value as the real thermal conductivity, but with a different dimension (m^2/s). We rebuild a temperature evolution equation

$$\tilde{\mathrm{g}}_i(\boldsymbol{x} + \boldsymbol{e}_i \delta t, t + \delta t) - \tilde{\mathrm{g}}_i(\boldsymbol{x}, t) = -\frac{1}{\tau_{\tilde{\mathrm{g}}}} \left[\tilde{\mathrm{g}}_i(\boldsymbol{x}, t) - \tilde{\mathrm{g}}_i^{eq}(\boldsymbol{x}, t)\right]. \tag{13}$$

The equilibrium distribution functions and the relaxation times in the temperature evolution equations for D2Q9 are:

$$\tilde{\mathrm{g}}_i^{eq} = \begin{cases} 0 & i = 0 \\ \frac{1}{6} T & i = 1 \; to \; 4 \\ \frac{1}{12} T & i = 5 \; to \; 8 \end{cases}, \tag{14}$$

$$\text{and } \tau_{\tilde{\mathrm{g}}} = \frac{3}{2} \frac{\tilde{\lambda}}{c^2 \delta t} + 0.5 , \tag{15}$$

for D3Q15, we have

$$\tilde{\mathrm{g}}_i^{eq} = \begin{cases} 0 & i = 0 \\ \frac{1}{9} T & i = 1 \; to \; 6 \\ \frac{1}{24} T & i = 7 \; to \; 14 \end{cases}, \tag{16}$$

and

$$\tau_{\tilde{\mathrm{g}}} = \frac{9}{5} \frac{\tilde{\lambda}}{c^2 \delta t} + 0.5 . \tag{17}$$

It is worth mentioning that the dimensions of these two sets of equilibrium distribution functions, Eq. (4) vs. Eq. (14) and Eq. (7) vs. Eq. (16), are different. As a result, the local macroscopic potential (T) and the flux (F) to the temperature diffusivity ($\tilde{\lambda}$) at each node are statistically calculated by

$$T = \sum_i \tilde{\mathrm{g}}_i , \tag{18}$$

$$\boldsymbol{F} = \left(\sum_i \boldsymbol{e}_i \tilde{\mathrm{g}}_i\right) \frac{\tau_{\tilde{\mathrm{g}}} - 0.5}{\tau_{\tilde{\mathrm{g}}}} . \tag{19a}$$

while the heat flux (q) in real space should be calculated by

$$\boldsymbol{q} = \left(\rho c_p \sum_i \boldsymbol{e}_i \tilde{\mathrm{g}}_i\right) \frac{\tau_{\tilde{\mathrm{g}}} - 0.5}{\tau_{\tilde{\mathrm{g}}}} . \tag{19b}$$

Note that the formula of heat flux differs from the previous works [40] as it depends not only on the temperature distribution function but also on the heat capacity of local phase. We

may have to calculate the heat flux at the interface to ensure continuous heat flux from both sides. After calculating the potential and the flux on each node, the effective temperature diffusivity $\tilde{\lambda}_{eff}$ can be determined by:

$$\tilde{\lambda}_{eff} = \frac{L \int \boldsymbol{F} \cdot dA}{\Delta T \int dA}, \tag{19c}$$

which is equal to the effective thermal conductivity demanded.

2.2 Revisit of PBB formulation for TCR

To account for the TCR within the LBM framework, a PBB scheme [40] was proposed by introducing a non-dimensional parameter δ whose value is within [0, 1], representing the bounced-back fraction of temperature distribution when trying to stream through the phase interface. Fig. 1(a) illustrates its simple idea that, at the interface only a fraction $(1-\delta)$ of the evolution quantity on a boundary node *I* of object Ω_1 can be propagated to the boundary node *J* of object Ω_2. Clearly, the adjacent boundary of two phases is completely insulated if $\delta = 1$; while the TCR is negligible if $\delta = 0$. Logically, if the TCR at an interface is non-negligible, then $0 < \delta < 1$. Thus, all the complicities in dealing with intricate interfacial contact are condensed into determining this single parameter δ.

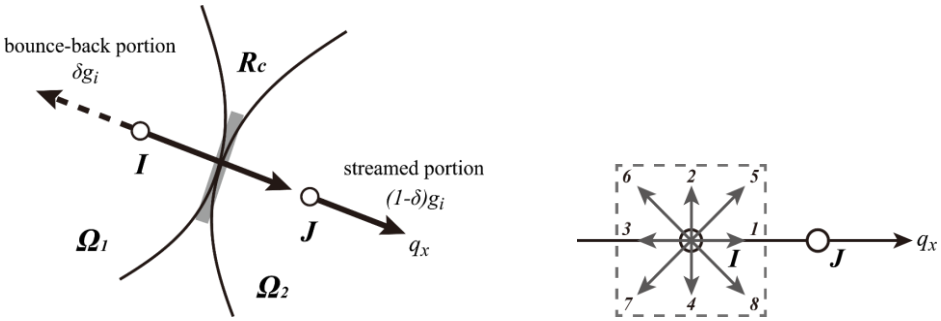

Fig. 1 (a) The schematic of the partial bounce-back scheme at interface: only a fraction (1-$\boldsymbol{\delta}$) of the streamed function can be propagated from one object (Ω_1) to the other (Ω_2). R_c is the thermal contact resistance. (b) A 1D heat conduction problem without thermal contact resistance, heat flows from the node *I* to node *J*.

The connection between this PBB parameter, δ, and the effective TCR, R_c, at two contacting phases was established by Han *et al* [40] using the continuity of heat flux at the interface as

$$R_c = \frac{3\delta}{1-\delta}. \tag{20}$$

This correlation looks simple and easy, and has been used for qualitative analysis of TCR effects on materials properties [40]. However, it is noticed that such a non-dimensional formula is hard to connect the predictions with practical applications, and as a result the quantitative investigation of TCR effects is unavailable. Therefore a reconsideration of this PBB scheme becomes necessary and demanded.

2.3 A corrected PBB scheme for dimensional TCR

Here, we are to correct the formula of dimensional TCR based on the PBB scheme. As no heat source is considered there, the existence of TCR may change the local temperature but not the continuity of heat flux. Considering the contact interface of two objects with the same

heat capacity (ρc_p), we re-derived and obtained the dimensional TCR as

$$R_c = \frac{3\delta}{\rho c_p (1-\delta) c} \quad , \tag{21}$$

where the dimension of R_c is correctly m^2K/W. Two main reasons might lead to the incorrect dimensionless formula of TCR in the previous work [40]: one was the incorrect expression of heat flux, and the other was the non-dimensional LBM framework used in Ref. [40] which led to the lattice speed c missing in the formula.

Further, if the heat capacities (ρc_p) of the two contact objects are different, we obtained a new dimensional TCR as

$$R_c = \frac{3\delta (T^I - T^J)}{[(\rho c_p)_1 T^I - (\rho c_p)_2 T^J](1-\delta) c} \quad , \tag{22}$$

where the subscripts "1" and "2" correspond to objects Ω_1 and Ω_2 respectively, the superscripts "I" and "J" correspond to the adjacent nodes I and J shown in Fig. 1(b). Detailed derivation process for Eq. (22) is presented in the Appendix.

This is an implicit scheme for TCR because R_c and the temperatures adjacent to the interface (T^I, T^J) influence each other. For two contact particles with different heat capacities, Eq. (22) indicates that the interface temperature cannot be eliminated from the formula as before. This is a bad news for us which brings much trouble for applications, and we are still putting efforts to find a better way to embed the dimensional TCR in the thermal LBM framework.

Therefore, in the present study hereafter, we are still focusing on the particle-reinforced composites with only one type of particles. Even though the liquid-solid interfacial thermal resistance exists, it is generally negligibly small compared with the solid-solid thermal contact resistance in composite systems. This work will demonstrate how the solid-solid TCR influences the effective thermal conductivity of the composite materials.

3. Results and discussion

Furthermore our simulation is confined in a domain with top and bottom as the isothermal boundaries and the surrounds as the insulated boundaries. For such given domain boundaries, we can follow the non-equilibrium bounce-back rule proposed by Zou and He [45] for the isothermal ones, and the Neumann method [24, 25] for the insulated ones, respectively.

3.1 Benchmarks

To validate the new dimensional PBB scheme, we compare the results for some simple cases already with known theoretical solutions. Consider pure steady-state heat conduction between two rectangular contacting solids with the same properties shown in Fig. 2 (a). Thermal conductivities of the solids are $\lambda_1 = \lambda_2 = 100\ W/(mK)$, and the width $h = 1\ m$. The top and bottom of the domain are isothermal at $T_1 = 100℃$ and $T_2 = 0℃$, and the left and right sides are insulated. Thence, the heat flux q and the effective thermal conductivity λ_{eff} have analytical solutions for a given TCR R_c.

In our simulations, we used 100 lattices in the vertical y direction, and the lattice space was 0.01 m consequently. To insure the value of τ_g within (0.5, 2), we set the lattice speed at

$c = 20000\,m/s$. For these given parameters, the PBB parameter δ can be calculated by Eq. (20) for any given R_c. Fig. 2 (b) shows the vertical temperature profiles for five different R_c. The temperature is continuous when $R_c = 0$ at the interface and no heat flux go through the interface when $R_c = \infty$. For finite R_c, the modeling results are compared with the analytical solutions in Table 1. Excellent agreements validate the derived dimensional PBB scheme within the thermal LBM framework.

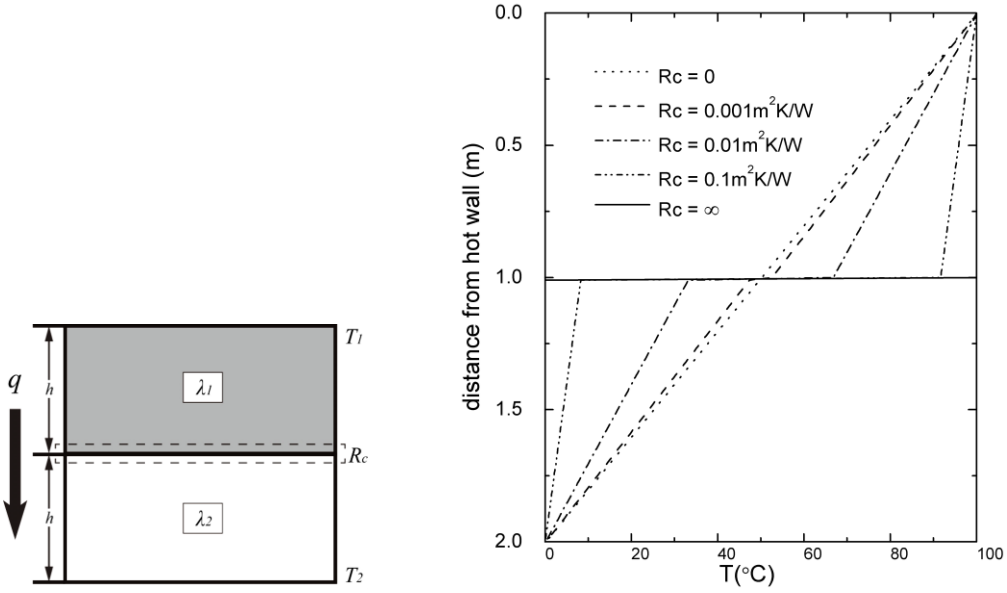

(a) **(b)**

Fig. 2 Validations of the modified PBB scheme. (a) Sketch of a pure steady state heat conduction problem between two rectangular contacting solids; (b) Temperature profiles in the y-direction for given different dimensional R_c.

Table 1 Comparisons between simulation results and analytical solutions for different R_c.

Parameters		Results			
		$q\ (W/m^2)$		$\lambda_{eff}\ (W/(mK))$	
$\boldsymbol{R_c\ (m^2K/W)}$	δ	Analytical values	Present simulations	Analytical values	Present simulations
0	0	5000	5000	100.00	100.00
0.001	$\frac{20}{23}$	4761.9	4761.9	95.238	95.238
0.01	$\frac{200}{203}$	3333.3	3333.3	66.667	66.667
0.1	$\frac{2000}{2003}$	833.33	833.33	16.667	16.667
1	$\frac{20000}{20003}$	98.039	98.039	1.9608	1.9608
∞	1	0.0000	0.0000	0.0000	0.0000

3.2 Applications for particle-reinforced composites

After validation, we use this scheme to predict the effective thermal property of particle-reinforced composites. Considering the random distribution and arbitrary geometry characteristics of particles in composites, we used the quartet structure generation set (QSGS) algorithms [26] to generate microstructures of the composites. Some generated structures with various particle volume fractions are shown in Fig. 3. Different from the previous work which used 0 or 1 to only recognize particle or matrix materials [38], we here assign each generated particle a unique number to distinguish it from others, so that we can recognize the interfaces between particles.

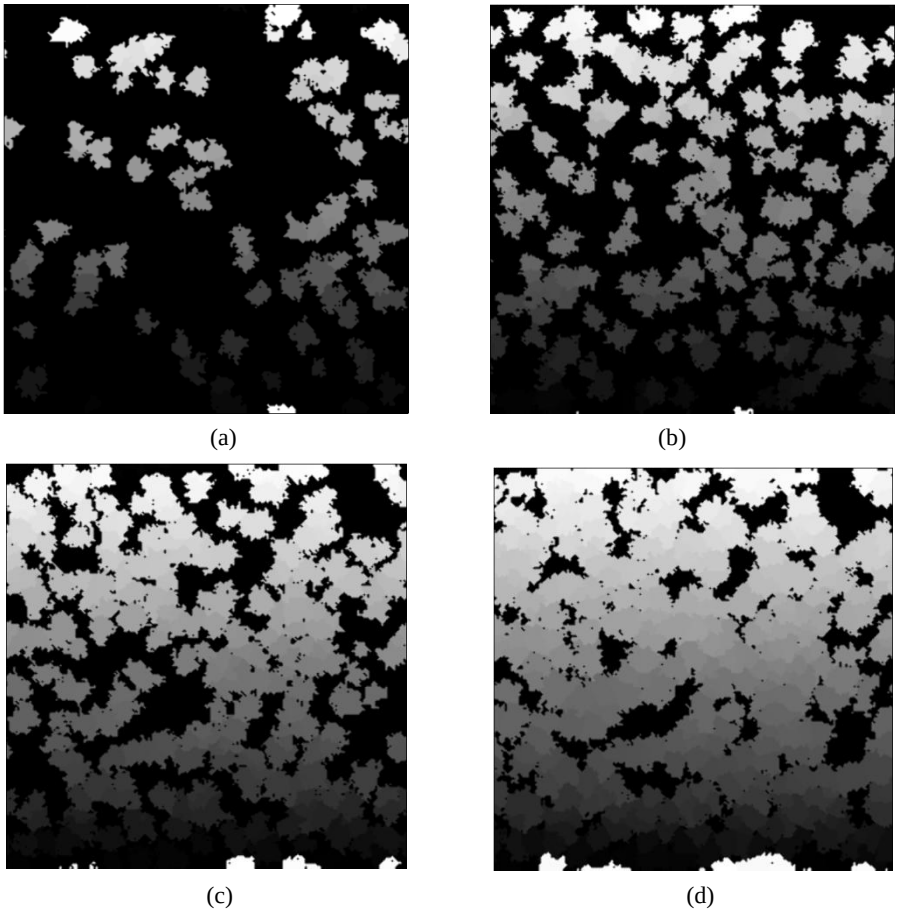

Fig. 3 Generated microstructures of particle-reinforced composites with different particle volume fractions φ by QSGS. (a) $\varphi = 0.2$. (b) $\varphi = 0.4$. (c) $\varphi = 0.6$. (d) $\varphi = 0.8$. The gray area represents particles and the pure black represents matrix phase. Each particle is given a number to be recognized. The domain is 2 mm×2 mm and the grid is 200×200. The averaged diameter of particles is d=10 μm.

Unless specified, the following simulations were performed in a two-dimensional 0.2 × 0.2 mm^2 domain on a 200×200 grid. The boundary temperatures are $T_1 = 10$ ℃ at the top and $T_2 = 0$ ℃ at the bottom, respectively. The left and right sides are adiabatic. The other simulation parameters include: the average diameter of particles $d = 10\,\mu m$, the thermal conductivities for matrix phase $\lambda_m = 1\ W/(mK)$ and for particles $\lambda_p = 100\ W/(mK)$, the lattice speed $c = 3 \times 10^8\ m/s$. We estimated the thermal contact resistance between particles at $R_c = 1 \times 10^{-6}\ m^2K/W$ by utilizing the Clausing and Chao's model [6], and neglected the thermal contact resistance between the particles and the low thermally

conductive matrix phase.

We studied the impact of R_c on the effective thermal conductivity of composites, λ_{eff}, for a given R_c value, $1 \times 10^{-6}\, m^2K/W$ at first, compared with the case without TCR, $R_c = 0$ as shown in Fig. 4 (a). TCR lowers the effective thermal conductivity and the TCR effect increases with the particle volume fraction. Significant deviations between the two cases are found once the particle volume fraction (φ) is higher than 0.5. The reason lies in the increased contact areas with rising φ value. When the particle volume fraction is very small (such as φ<0.3), the particle-particle contacts are quite rare, as shown in Fig. 3 (a), and therefore the effect of TCR is negligible. Fig. 4 (b) shows the temperature contours for the same geometry at φ=0.8 with or without TCR. When the TCR is not negligible ($R_c = 1 \times 10^{-6}\, m^2K/W$), the temperature contours are broken into finer pieces by the solid-solid contact interfaces and the temperature drop at each contact interface will reduce the overall thermal conductivity of the composite materials.

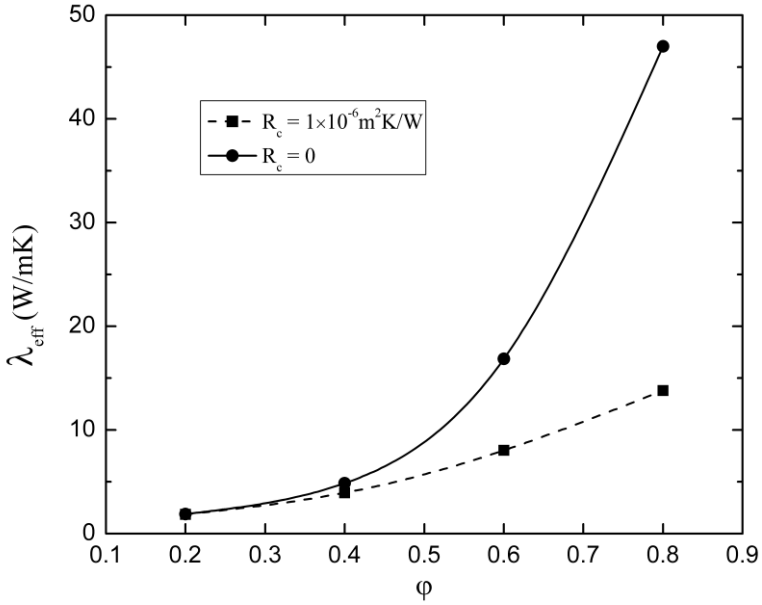

(a)

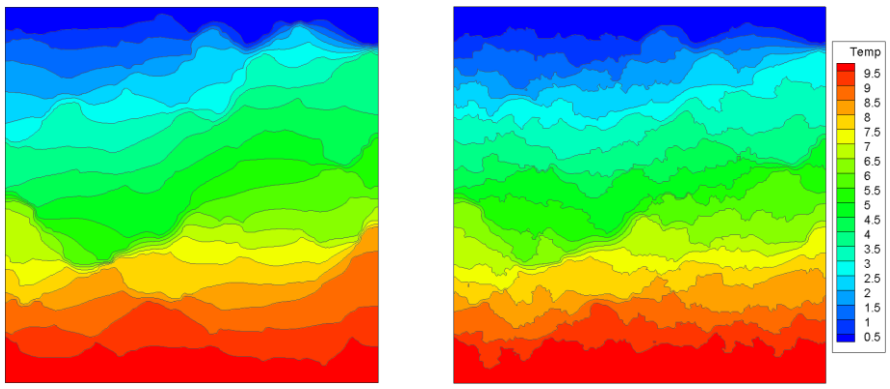

(without TCR) (with TCR)

(b)

Fig. 4 Thermal conductions for different particle volume fractions with ($R_c = 1 \times 10^{-6}\, m^2K/W$) or without ($R_c = 0$) thermal contact resistance. (a) Effective thermal conductivities; (b) Temperature contours at $\varphi = 0.8$.

For structure design of particle-reinforced composites, the size effect of particles on the

effective thermal conductivity is a significant issue. As stated before, the negligible TCR assumption, which is suitable for most macroscopic engineering materials [32, 33], leads to an increasing effective thermal conductivity with the decreased particle size at a given porosity [31]. However, for nanoporous materials such as in silica aerogels [35], experimental data has shown an opposite trend with the reduced particle size [34]. The increased number of interfaces for finer particles and thus non-negligible thermal resistance cause the conflicting results. By assuming the thermal contact resistance layers between particles as a gas layer network frame in the composite system, Wang et al. [38] obtained the same trend of particle size effect as the experiments of nanoporous materials. However assumption of uniform and constant contact resistance, equal to that of the matrix phase, limits the applicability of the method. Using the dimensional PBB scheme developed in this work, we can alter the value of TCR independently and the particle size, so as to re-examine the particle size effect on the overall effective thermal conductivity. The TCR value between particles varies from 0 to $1 \times 10^{-6}\ m^2K/W$, and we consider four statistically averaged diameters of particles of $d = 5, 10, 15$ or $20\ \mu m$. The solid particle fraction is φ = 0.8. Fig. 5 shows the effective thermal conductivity against the particle size, and mixed trends are shown. With a low thermal contact resistance, R_c, between solid particles, the effective thermal conductivity of composites, λ_{eff}, decreases with the increasing particle size, which agrees with the reported results from the engineering macroscopic materials. Conversely when R_c is beyond a certain level, $R_c > 10^{-8}\ m^2K/W$ in our simulations, λ_{eff} increases with the particle size. This means that if the thermal contact resistance is not negligible, the smaller the particles, the lower the effective thermal conductivity of composites for a given particle volume fraction. This trend agrees with the observations for nanoporous materials. Smaller particles increase the chance of particle-particle contact, hence denser interfaces, and more significant impact of TCR: this may provide a useful insight for designs and structure optimizations for nanomaterials.

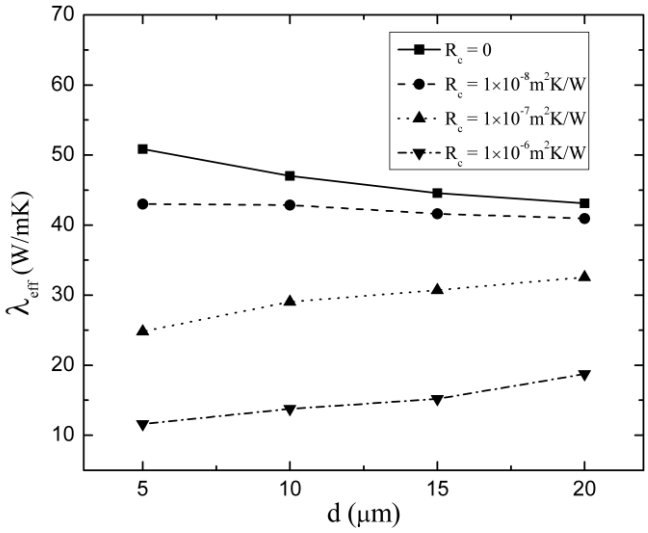

Fig. 5 Effect of particle size on composite effective thermal conductivity for different R_c at $\varphi = 0.8$.

4. Conclusions

To study the effective thermal conductivity of composite materials with thermal contact

resistance at particle-particle interfaces, we developed the partial bounce-back (PBB) scheme to include the thermal contact resistance at interfaces into the thermal lattice Boltzmann framework by re-deriving the redistribution function of heat at the phase interfaces for a corrected dimensional TCR formulation. The mechanism of simplified lattice Boltzmann scheme for solving the stead-state heat conduction equation is re-examined and revealed. After validation of the simulation results with the corresponding theoretical solution for a simple case, we applied this new method to the effective thermal conductivities of composite materials where the contract thermal resistance was not negligible, and demonstrated the effects of the particle volume fraction, the value of thermal contact resistance and the particle size. The results showed that (1) the existence of TCR lowered the effective thermal conductivity and the TCR effect increased with the particle-particle interfaces; (2) the connection between the effective thermal conductivity and particle size is complex. With a low thermal contact resistance, the effective thermal conductivity of composites decreased with the increasing particle size, which agreed with the facts in macroscopic engineering materials. However if the thermal contact resistance was not negligible, a smaller average size of particles led to a lower effective thermal conductivity of composites for a given volume fraction, which agreed with the observations for nanoporous materials.

Acknowledgements: This work is financially supported by the NSFC grant (No. 51176089), the Specialized Research Fund for the Doctoral Program of Higher Education of China (No. 20130002110077) and the startup funding for the Recruitment Program of Global Young Experts of China.

Appendix: Derivation of the dimensional TCR

Here we present the details in obtaining Eqs. (21) and (22) for the dimensional TCR.

For the system shown in Fig. 1(a), the thermal contact resistance R_c can be obtained from subtraction of the total thermal resistance R_T between nodes *I* and *J* and the thermal resistance per lattice grid R_{g} as

$$R_c = R_T - R_{\mathrm{g}} . \tag{A1}$$

Since the thermal resistance is defined as

$$R = \frac{\Delta T}{q} = \frac{T^I - T^J}{q} , \tag{A2}$$

we need to find the relation between the temperature difference and heat flux from node *I* to *J* for R_T and R_{g} respectively.

In order to get the lattice gird resistance R_{g}, we consider a 1D heat conduction problem as shown in Fig. 1(b). Heat flows from node *I* to *J*. For steady state, we can establish the following relations for the temperature distribution functions:

$$\tilde{\mathrm{g}}_2 = \tilde{\mathrm{g}}_4 = \tilde{\mathrm{g}}_2^{eq} = \frac{1}{6}T; \quad \tilde{\mathrm{g}}_5 = \tilde{\mathrm{g}}_8 ; \quad \tilde{\mathrm{g}}_6 = \tilde{\mathrm{g}}_7 , \tag{A3}$$

Based on Eq. (19), the axial heat flux is calculated as

$$q_x = (\rho c_p)_1 \left(\sum e_{\alpha,\mathrm{x}} \tilde{\mathrm{g}}_\alpha^I\right) \frac{\tau_{\tilde{\mathrm{g}}} - 0.5}{\tau_{\tilde{\mathrm{g}}}} = (\rho c_p)_2 \left(\sum e_{\alpha,\mathrm{x}} \tilde{\mathrm{g}}_\alpha^J\right) \frac{\tau_{\tilde{\mathrm{g}}} - 0.5}{\tau_{\tilde{\mathrm{g}}}} . \tag{A4}$$

Denoting $q_x' = \rho c_p \sum e_{\alpha,\mathrm{x}} \tilde{\mathrm{g}}_\alpha$, we have

$$q_x' = (\rho c_p)_1 e\left[\tilde{g}_1^I - \tilde{g}_3^I + 2\left(\tilde{g}_5^I - \tilde{g}_7^I\right)\right] = (\rho c_p)_2 e\left[\tilde{g}_1^J - \tilde{g}_3^J + 2\left(\tilde{g}_5^J - \tilde{g}_7^J\right)\right]. \tag{A5}$$

By using Eq. (A3), the temperature at node *I* is

$$\frac{2}{3}T^I = \tilde{g}_1^I + \tilde{g}_3^I + 2\left(\tilde{g}_5^I + \tilde{g}_7^I\right). \tag{A6}$$

Combining Eqs. (A5) and (A6) gives

$$\begin{cases} \tilde{g}_1^I + 2\tilde{g}_5^I = \dfrac{1}{3}T^I + \dfrac{1}{2}\dfrac{q_x'}{e(\rho c_p)_1} \\ \tilde{g}_3^I + 2\tilde{g}_7^I = \dfrac{1}{3}T^I - \dfrac{1}{2}\dfrac{q_x'}{e(\rho c_p)_1} \end{cases}. \tag{A7}$$

Similarly, for node *J* :

$$\begin{cases} \tilde{g}_1^J + 2\tilde{g}_5^J = \dfrac{1}{3}T^J + \dfrac{1}{2}\dfrac{q_x'}{e(\rho c_p)_2} \\ \tilde{g}_3^J + 2\tilde{g}_7^J = \dfrac{1}{3}T^J - \dfrac{1}{2}\dfrac{q_x'}{e(\rho c_p)_2} \end{cases}. \tag{A8}$$

According to the evolution equation of the temperature distribution functions, we get

$$\begin{cases} (\rho c_p)_2\, \tilde{g}_1^J = (\rho c_p)_1[\tilde{g}_1^I - \dfrac{1}{\tau_{\tilde{g}}}\left(\tilde{g}_1^I - \dfrac{1}{6}T^I\right)] \\ (\rho c_p)_2\, \tilde{g}_5^J = (\rho c_p)_1[\tilde{g}_5^I - \dfrac{1}{\tau_{\tilde{g}}}\left(\tilde{g}_5^I - \dfrac{1}{12}T^I\right)] \end{cases}. \tag{A9}$$

By substituting Eq. (A9) into Eqs. (A7) and (A8),

$$q_x' = \frac{2e\tau_{\tilde{g}}}{3}[\left(\rho c_p\right)_1 T^I - \left(\rho c_p\right)_2 T^J], \tag{A10}$$

and

$$q_x = \frac{\tau_{\tilde{g}} - 0.5}{\tau_{\tilde{g}}} q_x' = \frac{2e}{3}(\tau_{\tilde{g}} - 0.5)\,[\left(\rho c_p\right)_1 T^I - \left(\rho c_p\right)_2 T^J], \tag{A11}$$

Based on the definition, the thermal resistance per lattice grid R_g is

$$R_g = \frac{\Delta T}{q_x} = \frac{3(T^I - T^J)}{2e(\tau_{\tilde{g}} - 0.5)\,[\left(\rho c_p\right)_1 T^I - \left(\rho c_p\right)_2 T^J]}. \tag{A12}$$

Next, we need to obtain the total thermal resistance R_T between nodes *I* and *J* for the system shown in Fig. 1(a). Multiplying the temperature distribution function $\tilde{g}$ by the heat capacity (ρc_p), and based on the PBB scheme mentioned in Section 2.2, we recover the energy redistribution correlation as

$$\begin{cases} \left(\rho c_p\right)_1 \tilde{g}_3^I = \left(\rho c_p\right)_1 \delta \breve{g}_1^I + \left(\rho c_p\right)_2 (1-\delta)\breve{g}_3^J & \text{(A13a)} \\ \left(\rho c_p\right)_1 \tilde{g}_7^I = \left(\rho c_p\right)_1 \delta \breve{g}_5^I + \left(\rho c_p\right)_2 (1-\delta)\breve{g}_7^J \ , & \text{(A13b)} \end{cases}$$

where

$$\begin{cases} \breve{g}_1^I = \tilde{g}_1^I - \dfrac{1}{\tau_{\tilde{g}}}\left(\tilde{g}_1^I - \dfrac{1}{6}T^I\right) & \text{(A14a)} \\ \breve{g}_5^I = \tilde{g}_5^I - \dfrac{1}{\tau_{\tilde{g}}}\left(\tilde{g}_5^I - \dfrac{1}{12}T^I\right) & \text{(A14b)} \\ \breve{g}_3^J = \tilde{g}_3^J - \dfrac{1}{\tau_{\tilde{g}}}\left(\tilde{g}_3^J - \dfrac{1}{6}T^J\right) & \text{(A14c)} \\ \breve{g}_7^J = \tilde{g}_7^J - \dfrac{1}{\tau_{\tilde{g}}}\left(\tilde{g}_7^J - \dfrac{1}{12}T^J\right) & \text{(A14d)} \end{cases}$$

are the post-collision temperature distribution functions.

Combining Eqs. (A14a) and (A14b) leads to

$$\breve{g}_1^I + 2\breve{g}_5^I = \left(1 - \frac{1}{\tau_{\tilde{g}}}\right)\left(\tilde{g}_1^I + 2\tilde{g}_5^I\right) + \frac{T^I}{3\tau_{\tilde{g}}}. \quad \text{(A15a)}$$

Similarly, for node *J*:

$$\breve{g}_3^J + 2\breve{g}_7^J = \left(1 - \frac{1}{\tau_{\tilde{g}}}\right)\left(\tilde{g}_3^J + 2\tilde{g}_7^J\right) + \frac{T^J}{3\tau_{\tilde{g}}}. \quad \text{(A15a)}$$

Summing Eqs. (A13a) and (A13b) and using Eq. (A7) give

$$\tilde{g}_3^I + 2\tilde{g}_7^I = \delta\left(\breve{g}_1^I + 2\breve{g}_5^I\right) + \frac{\left(\rho c_p\right)_2}{\left(\rho c_p\right)_1}(1-\delta)\left(\breve{g}_3^J + 2\breve{g}_7^J\right) = \frac{1}{3}T^I - \frac{1}{2}\frac{q_x'}{e\left(\rho c_p\right)_1}. \quad \text{(A16)}$$

Substituting Eq. (A15) into Eq.(A16), we have

$$q_x' = \frac{1-\delta}{3}\frac{\tau_{\tilde{g}}}{\delta\left(\tau_{\tilde{g}} - 1\right) + 0.5}\, e\left[\left(\rho c_p\right)_1 T^I - \left(\rho c_p\right)_2 T^J\right], \quad \text{(A17)}$$

and

$$q_x = \frac{\tau_{\tilde{g}} - 0.5}{\tau_{\tilde{g}}} q_x' = \frac{1-\delta}{3\delta\left(\tau_{\tilde{g}} - 1\right) + 1.5} e\left(\tau_{\tilde{g}} - 0.5\right)\left[\left(\rho c_p\right)_1 T^I - \left(\rho c_p\right)_2 T^J\right]. \quad \text{(A18)}$$

Based on Eq. (A2), the total thermal resistance R_T is

$$R_T = \frac{3\delta(T^I - T^J)}{e(1-\delta)\left[\left(\rho c_p\right)_1 T^I - \left(\rho c_p\right)_2 T^J\right]} + \frac{3(T^I - T^J)}{2e(\tau_{\tilde{g}} - 0.5)\left[\left(\rho c_p\right)_1 T^I - \left(\rho c_p\right)_2 T^J\right]}. \quad \text{(A19)}$$

Finally, by substituting Eqs. (A12) and (A19) into Eq. (A1), the thermal contact resistance R_c is obtained, as the form of Eq. (22).

References

[1] V. Sartre, M. Lallemand, Enhancement of thermal contact conductance for electronic systems, Applied Thermal Engineering, 21 (2001) 221-235.

[2] M. Grujicic, C.L. Zhao, E.C. Dusel, The effect of thermal contact resistance on heat management in the electronic packaging, Applied Surface Science, 246 (2005) 290-302.

[3] D.P.H. Hasselman, L.F. Johnson, Effective Thermal Conductivity of Composites with Interfacial Thermal Barrier Resistance, Journal of Composite Materials, 21 (1987) 508 -515.

[4] C.-W. Nan, R. Birringer, D.R. Clarke, H. Gleiter, Effective thermal conductivity of particulate composites with interfacial thermal resistance, Journal of Applied Physics, 81 (1997) 6692-6699.

[5] M.R. Sridhar, M.M. Yovanovicht, Review of elastic and plastic contact conductance models: comparison with experiment, Journal of Thermophysics and Heat Transfer, 8 (1994) 633-640.

[6] A.M. Clausing, B.T. Chao, Thermal Contact Resistance in a Vacuum Environment, Journal of Heat Transfer, 87 (1965) 243-250.

[7] M. Bahrami, J.R. Culham, M.M. Yananovich, G.E. Schneider, Review of thermal joint resistance models for nonconforming rough surfaces, Applied Mechanics Reviews, 59 (2006) 1-12.

[8] S. Chen, G.D. Doolen, Lattice boltzmann method for fluid flows, Annual Review of Fluid Mechanics, 30 (1998) 329-364.

[9] C.K. Aidun, J.R. Clausen, Lattice-Boltzmann method for complex flows, Annual Review of Fluid Mechanics, 42 (2010) 439-472.

[10] S. Chen, H. Chen, D. Martnez, W. Matthaeus, Lattice Boltzmann model for simulation of magnetohydrodynamics, Physical Review Letters, 67 (1991) 3776-3779.

[11] D.O. Martinez, C. Shiyi, W.H. Matthaeus, Lattice Boltzmann thermohydrodynamics, Physics of plasmas, 1 (1994) 1850-1867.

[12] X. He, N. Li, Lattice Boltzmann simulation of electrochemical systems, Computer Physics Communications, 129 (2000) 158-166.

[13] G. Breyiannis, D. Valougeorgis, Lattice kinetic simulations in three-dimensional magnetohydrodynamics, Physical Review E, 69 (2004) 065702.

[14] J. Wang, M. Wang, Z. Li, Lattice Boltzmann simulations of mixing enhancement by the electro-osmotic flow in microchannels, Modern Physics Letters B, 19 (2005) 1515-1518.

[15] Z. Guo, T.S. Zhao, Y. Shi, A lattice Boltzmann algorithm for electro-osmotic flows in microfluidic devices, The Journal of Chemical Physics, 122 (2005) -.

[16] J. Wang, M. Wang, Z. Li, Lattice Poisson–Boltzmann simulations of electro-osmotic flows in microchannels, Journal of Colloid and Interface Science, 296 (2006) 729-736.

[17] M. Wang, Q. Kang, Electrokinetic transport in microchannels with random roughness, Analytical Chemistry, 81 (2009) 2953-2961.

[18] F.J. Alexander, S. Chen, J.D. Sterling, Lattice Boltzmann thermohydrodynamics, Physical Review E, 47 (1993) R2249-R2252.

[19] G. McNamara, B. Alder, Analysis of the lattice Boltzmann treatment of hydrodynamics, Physica A: Statistical Mechanics and its Applications, 194 (1993) 218-228.

[20] Y. Chen, H. Ohashi, M. Akiyama, Thermal lattice Bhatnagar-Gross-Krook model without nonlinear deviations in macrodynamic equations, Physical Review E, 50 (1994) 2776-2783.

[21] X. Shan, Simulation of Rayleigh-Bénard convection using a lattice Boltzmann method, Physical Review E, 55 (1997) 2780-2788.

[22] J.G.M. Eggels, J.A. Somers, Numerical simulation of free convective flow using the

lattice-Boltzmann scheme, International Journal of Heat and Fluid Flow, 16 (1995) 357-364.
[23] X. He, S. Chen, G.D. Doolen, A novel thermal model for the lattice Boltzmann method in incompressible limit, Journal of Computational Physics, 146 (1998) 282 - 300.
[24] Y. Peng, C. Shu, Y.T. Chew, Simplified thermal lattice Boltzmann model for incompressible thermal flows, Physical Review E, 68 (2003) 026701.
[25] J. Wang, M. Wang, Z. Li, A lattice Boltzmann algorithm for fluid-Csolid conjugate heat transfer, International Journal of Thermal Sciences, 46 (2007) 228-234.
[26] M. Wang, J. Wang, N. Pan, S. Chen, Mesoscopic predictions of the effective thermal conductivity for microscale random porous media, Physical Review E, 75 (2007) 036702.
[27] M. Wang, J. He, J. Yu, N. Pan, Lattice Boltzmann modeling of the effective thermal conductivity for fibrous materials, International Journal of Thermal Sciences, 46 (2007) 848-855.
[28] M. Wang, J. Wang, N. Pan, S. Chen, J. He, Three-dimensional effect on the effective thermal conductivity of porous media, Journal of Physics D:Applied Physics, 40 (2007) 260-265.
[29] M. Wang, Q. Kang, N. Pan, Thermal conductivity enhancement of carbon fiber composites, Applied Thermal Engineering, 29 (2009) 418-421.
[30] M. Wang, N. Pan, Modeling and prediction of the effective thermal conductivity of random open-cell porous foams, International Journal of Heat and Mass Transfer, 51 (2008) 1325-1331.
[31] M.R. Wang, N. Pan, J.K. Wang, S.Y. Chen, Mesoscopic simulations of phase distribution effects on the effective thermal conductivity of microgranular porous media, Journal of Colloid and Interface Science, 311 (2007) 562-570.
[32] K. Midttomme, E. Roaldset, The effect of grain size on thermal conductivity of quartz sands and silts, Petroleum Geoscience, 4 (1998) 165-172.
[33] J.Z. Liang, F.H. Li, Measurement of thermal conductivity of hollow glass-bead-filled polypropylene composites, Polymer Testing, 25 (2006) 527-531.
[34] F.X. Alvarez, D. Jou, A. Sellitto, Pore-size dependence of the thermal conductivity of porous silicon: A phonon hydrodynamic approach, Applied Physics Letters, 97 (2010) 033103-033103-033103.
[35] J.J. Zhao, Thermophysical Properties and Heat Transfer Mechanisms of Microscale and Nanoscale Structures in Aerogel-based Composite Insulators, in: Thermal Engineering, Vol. Ph.D, Tsinghua University, Beijing, China, 2012.
[36] L. Gailite, P.E. Scopelliti, V.K. Sharma, M. Indrieri, A. Podestà, G. Tedeschi, P. Milani, Nanoscale Roughness Affects the Activity of Enzymes Adsorbed on Cluster-Assembled Titania Films, Langmuir, 30 (2014) 5973-5981.
[37] X. Ma, X. Qu, Q. Zhang, F. Chen, Analysis of interfacial action of rectorite/thermoplastic polyurethane nanocomposites by inverse gas chromatography and molecular simulation, Polymer, 49 (2008) 3590-3600.
[38] M. Wang, X.M. Wang, J.K. Wang, N. Pan, Grain size effects on effective thermal conductivity of porous materials with internal thermal contact resistance, Journal of Porous Media, 16 (2013) 1043-1048.
[39] H. Yoshida, T. Kobayashi, H. Hayashi, T. Kinjo, H. Washizu, K. Fukuzawa, Boundary condition at a two-phase interface in the lattice Boltzmann method for the convection-diffusion equation, Physical Review E, 90 (2014) 013303.
[40] K. Han, Y.T. Feng, D.R.J. Owen, Modelling of thermal contact resistance within the framework of the thermal lattice Boltzmann method, International Journal of Thermal Sciences, 47 (2008) 1276-1283.

[41] M. Wang, N. Pan, Predictions of effective physical properties of complex multiphase materials, Materials Science and Engineering: R: Reports, 63 (2008) 1-30.
[42] A. D Orazio, S. Succi, Boundary Conditions for Thermal Lattice Boltzmann SimulationsComputational Science, Computer Science, 2657 (2003) 656-656.
[43] X. Chen, P. Han, A note on the solution of conjugate heat transfer problems using SIMPLE-like algorithms, International Journal of Heat and Fluid Flow, 21 (2000) 463–467.
[44] M. Wang, N. Pan, J. Wang, S. Chen, Mesoscopic simulations of phase distribution effects on the effective thermal conductivity of microgranular porous media, Journal of Colloid and Interface Science, 311 (2007) 562-570.
[45] Q. Zou, X. He, On pressure and velocity boundary conditions for the lattice Boltzmann BGK model, Physics of Fluids, 9 (1997) 1591-1598.